ELSEVIER

Contents lists available at ScienceDirect

Bioresource Technology

journal homepage: www.elsevier.com/locate/biortech





Effect of solvent and feedstock selection on primary and secondary chars produced via hydrothermal carbonization of food wastes

Matteo Pecchi ^{a,b}, Marco Baratieri ^b, Jillian L. Goldfarb ^{a,*}, Alex R. Maag ^a

- ^a Department of Biological & Environmental Engineering, College of Agriculture and Life Sciences, Cornell University, USA
- ^b Faculty of Science and Technology, Free University of Bolzano, Italy

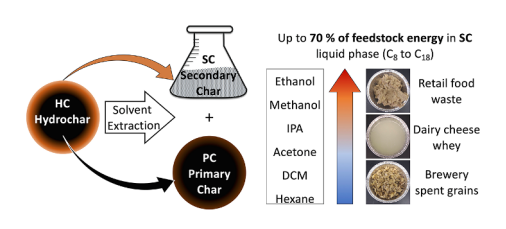
HIGHLIGHTS

- Hydrothermal carbonization converts various food wastes into hydrochar.
- Hydrochars are separated into primary and secondary char using six solvents.
- Primary char has coal-like characteristics, secondary char is an oily phase.
- Lipids are recovered in secondary char and can be upgraded to a liquid fuel.
- Ethanol maximizes secondary char mass and primary char fixed carbon fraction.

ARTICLE INFO

Keywords:
Hydrothermal Carbonization
HTC
Solvent extraction
Hydrochar
Secondary Char
Food Waste

GRAPHICAL ABSTRACT



ABSTRACT

Hydrothermal carbonization is a thermochemical process that converts wet waste biomass into hydrochar, a renewable solid fuel that comprises a coal-like primary phase and an oily secondary phase. The varying oxidation rates of these phases may result in an inefficient energy recovery when combusting the hydrochar, as secondary char is more reactive. Brewer's spent grain, dairy cheese whey and food waste were hydrothermally carbonized at 250 °C. The hydrochars were extracted using six solvents to evaluate the hydrochar partitioning between primary and secondary char phases. Feedstock nature and solvent selection impact the amount and composition of these phases detected. For lipid-rich feedstocks, ethanol extracts up to 50 wt% secondary char enriched in liquid fuel precursors from a solid primary char with enhanced coal-like characteristics. For substrates rich in carbohydrates, proteins, and lignocellulose, less secondary char is produced. Acetone and dichloromethane remove the oily secondary char and maximize primary char yield.

1. Introduction

The U.S. landfilled 35 million of the over 70 million tons of food waste produced in 2018 (Environment Protection Agency, 2018). Landfilled food waste generates greenhouse gas emissions during decomposition and potentially toxic leachates as rainwater percolates through the landfill. Hydrothermal carbonization (HTC) is a promising management strategy to convert wet biomasses such as food waste into a renewable solid fuel.

HTC is a thermochemical process where a carbonaceous substrate is heated between 180 and 250 °C under (usually) autogenous pressure in aqueous media. During HTC, the solid feed undergoes a series of dehydration, hydrolysis, decarboxylation, and decarbonylation reactions to create water-soluble organic products and a gas phase largely comprised of CO₂ (Libra et al., 2011). The remaining solid carbonizes into a solid hydrochar (HC), a coal-like material with potential applications as soil amendments (Hitzl et al., 2018), adsorbents, (Zhang et al., 2019) activated carbon precursors (Jain et al., 2016), and renewable solid fuels

 $\hbox{\it E-mail addresses: goldfarb@cornell.edu, JillianLGoldfarb@gmail.com, JillianLGoldfarb@gmail.com (J.L.~Goldfarb).}$

https://doi.org/10.1016/j.biortech.2022.126799

^{*} Corresponding author.

(Mihajlović et al., 2018).

The composition and thermophysical properties of HC depend on the feedstock properties and processing conditions (Lucian et al., 2018), which in turn guide the HC's end-use application. Several hydrothermal carbonization studies have identified positive energy recoveries using HCs as a solid fuel. For example, under certain processing conditions, Danso-Boateng et al. (Danso-Boateng et al., 2015) estimated a net energy generation of 600 kJ/kg using an 85% moisture fecal feedstock. HTC also reduces the ash content in the HC compared to the raw feedstock, improving the suitability of HC for use as a solid fuel (Liu et al., 2014; Sharma and Dubey, 2020).

HCs comprise two phases; a primary char (PC) phase produced from solid-solid carbonization reactions within the original solid feedstock matrix and a secondary char (SC) phase formed at the solid-liquid interface via aqueous phase (re)polymerization and condensation reactions. The secondary char phase often condenses on the PC surface as spheres. Prior work demonstrates the extractability of secondary char using of a mixture of methanol and acetone as the solvent (Lucian et al., 2018; Volpe et al., 2018).

Owing to a lack of systematic analysis of the effect of solvent selection on the extraction of SC from HCs, it is difficult to gauge whether the condensed phase is best separated to reclaim potential biofuel precursors, or if the as-carbonized HC should be used as a solid fuel. Prior literature demonstrates a high pyrolytic and oxidative reactivity of HCs, which could result in early burn-out and inefficient combustion processes (Gao et al., 2019). The objective of this work is to assess the interplay between feedstock composition and solvent selection on the extractability of SC and the properties of PC and SC produced from HTC of three biomass feedstocks available at an industrial scale: food waste, dairy cheese whey, and brewer's spent grain. Such fundamental data will shed insight into how each char phase influences the apparent properties of the HC product and the potential to isolate products as a function of solvent selection.

2. Materials and methods

2.1. Feedstocks

A representative retail-level food waste was created by weighing and mixing the ingredients shown in Table 1 (Buzby Jean et al., 2014) in a

Table 1Composition of SRU feedstock moisture used for HTC.

Food Waste Category	Composition [wt %]	Products used (equal quantities, by mass, of each item were used for each category)		
Grain products	16.7	Rice, dry pasta, bread, biscuits, harvest wheat crackers, plain bagels		
Fresh fruit	10.2	Banana, apples, tangerines, strawberries, grapes		
Processed fruit	3.7	Raspberry jam, applesauce, seedless raisins		
Fresh vegetables	12.1	Iceberg lettuce, baking potatoes, carrots, bell pepper, broccoli		
Processed vegetables	4.2	Canned sweet peas, corn, kidney beans, tomato sauce		
Milk	15.1	2% milk		
Dairy (not milk)	6.5	Plain low-fat yogurt, cheddar cheese, small curd cottage cheese		
Meat	3.3	Ground beef, uncured bacon		
Poultry	2.1	Chicken (whole rotisserie), breaded chicken nuggets		
Fish and seafood	0.9	Canned tuna, fresh salmon, raw shrimp, pre- frozen tilapia		
Eggs	1.6	Grade AA large eggs		
Nuts	0.5	Lightly salted dry roasted peanuts		
Sweeteners	10.5	Pepsi, Hostess cupcakes, candy (KitKat), raw sugar cookie dough		
Fats and oils	12.6	Beef tallow, all-vegetable shortening, canola oil		
Total	100.0			

household blender. The mixture represents typical food waste from producers like Supermarkets, Restaurants, and Universities and is therefore named SRU. Dairy cheese whey (DCW), a semi-transparent aqueous waste from the cheese production process, was sourced from the Cornell University Dairy. Brewers' spent grains (BSG) were obtained from a local brewery in Ithaca, NY, USA. Each material was preserved in a freezer at $-4^{\circ}\mathrm{C}$ and defrosted just prior to experiments. The moisture content of each feedstock was assessed gravimetrically by repeated drying in a laboratory oven at 90 °C until constant weight was reached in at least triplicate measurements. A portion of each feedstock was dried for further analyses and solvent extraction.

2.2. Hydrothermal carbonization of feedstocks

HTC was performed using a 1-liter Parr reactor. For each run, the reactor was loaded with the substrate and then water was added to reach a biomass/water ratio of 0.15. The only exception was DCW which was used as-received, with a biomass to water ratio of 0.05. A reactor filling ratio of 0.5 was adopted, which meant approximately 500 g of material (water included) were used in each run. Before the run, the reactor was purged 3 times with high purity nitrogen (Airgas) and then pressurized to 0.55-0.58 MPa. The impeller speed was set to 400 rpm. The reactor was heated to 250 °C and held for 1 h (the timer was started when the reactor temperature reached the setpoint minus a threshold of 2.5%). The ramp time was between 120 and 134 min for all cases except the run with DCW, which lasted only 97 min (likely due to the higher water content and therefore lower heat capacity of the substrate). The reactor was quenched in an ice bath, reaching a temperature of 70 °C in about 5 min. The reactor was further cooled to 20 °C, then the gas was purged, and the reactor was opened. The liquid and solid slurry was vacuum filtered on 45 µm ashless cellulose filter paper. The HC was oven dried at 85 °C for at least 24 h and stored in plastic containers. The HC yield was obtained as the dry mass of HC divided by the dry feedstock mass. The liquid yield was obtained by subtracting the final mass of liquid by the initial water and the feedstock moisture and dividing the results by the dry feedstock mass. The gas was considered to be 100% CO₂ (Libra et al., 2011) and its mass was obtained using Eq. (1), where $P_{initial}$ and $P_{cooling}$ are the pressure in the reactor before HTC and after cooling the reactor to a temperature value of $T_{cooling}$, $V_{reactor}$ is the reactor volume and $f_{filling}$ is the fraction occupied by the feedstock, MM_{CO_2} is the molar mass of CO_2 , and R_{gas} is the universal gas constant. To obtain the gas yield, m_{gas} was divided by the dry feedstock mass. The reactor was also weighed after degassing on a 5-gram precision scale as a check for the computed gas value. Losses were calculated as 100 % minus the sum of HC, liquid, and

$$m_{gas} = (P_{cooling} - P_{initial}) \cdot (V_{reactor} \cdot f_{filling}) \cdot \frac{MM_{CO_2}}{R_{onv} \cdot T_{cooling}}$$
(1)

2.3. Hydrochar solvent extraction

Six different solvents were used to extract the SC from the HCs: isopropyl alcohol (IPA, 99 % purity from Ward's Science), methanol (MET, 99.8 % purity from Alfa Aesar), ethanol (ETH, 200 Proof from Decon Labs, Inc), acetone (ACE, HPLC purity from Fisher Chemical), dichloromethane (DCM, 98 % purity from Acros Organics), and hexanes (HEX, HPLC purity from Fisher Chemical). For each sample, 0.3 g of HC were loaded into a vial (V1) with 10 mL of solvent and shaken for 3 h. After shaking, the contents were poured over ashless cellulose filter paper through a glass funnel, then another 10 mL aliquot of solvent was poured into V1, rinsed, then poured through the sample on the filter paper. The filtrate was collected in another vial (V2), held in a cold bath. After filtration, the filter paper and its contents were placed inside V1, which was then oven or air dried in a fume hood, depending on the solvent flammability. A few mL from V2 were air dried in an aluminum boat, then V2 was capped and stored at 4 °C. The untreated

(unextracted) solid phase is referred to as HC, the post-extraction solid dried residue inside V1 as primary char (PC), and the extracted material, in its dry form inside the aluminum boats or solubilized in the solvent inside V2, as secondary char (SC). The fraction of PC was obtained by gravimetric analysis, while the SC recovery was determined by difference of as-carbonized HC minus PC.

2.4. Analysis of chars

Proximate analysis of HC and PC samples was performed through thermogravimetric analysis (TGA) using a TA Instruments Simultaneous Thermal Analyzer 650 and a TA Instruments TGA 5500. Approximately 5 mg of sample was heated to 110 $^{\circ}$ C in high purity N₂ (100 mL/min for the 650 TGA, 20 mL/min for the 5500 TGA, scaled by the considerably reduced volume of the 5550 vs 650 instruments per manufacture's recommendation) and held for at least 30 min to remove moisture. Then the temperature was raised to 900 $^{\circ}\text{C}$ at 10 $^{\circ}\text{C}$ min and held constant for 60 min; loss is attributed to volatile matter (VM). The gas flow of N_2 was then switched to dry air, while the temperature was increased to 925 $^{\circ}\text{C}$ while heated at the same rate, 10 °C/min, and held for 60 min. Oxidizable matter lost over this step is the fixed carbon (FC). Residual mass is loosely termed "ash". The reproducibility between the two instruments was checked running some of the samples on both TGAs and comparing the results, which were within 5 %. Proximate analyses were performed at least in duplicates.

Ultimate analysis of the HC and PC was performed using a Vario MACRO Cube (Elementar) elemental analyzer, calibrated using sulfanilamide. For each char sample, carbon, hydrogen, and nitrogen content were measured in triplicate. Oxygen was determined by difference.

The Higher Heating Values (HHV) of the dried HC samples were obtained using a 6200 Isoperibol Calorimeter equipped with a 6510 Water Handling system, Parr, USA. The combustion vessels were calibrated using benzoic acid pellets. Each HHV measurement was performed in triplicate. Since primary and secondary char quantities were too small to evaluate their HHV using the 6200 Isoperibol Calorimeter, for energy recovery determination, their HHV values were estimated using Dulong's formula, in MJ/kg:

 $HHV = 0.338 \bullet \text{ [C]} + 1.428 \bullet \text{ ([H]} - 1/8 \text{[O]) (2)}$

The [C], [H] and [O] values are carbon, hydrogen and oxygen elemental contents, respectively. The Energy recovery (ER) of the HC was then calculated using the following formula:

 $ER = Y_{HC} \cdot HHV_{HC} / HHV_{Feed} \cdot 100\%$ (3)

Where Y_{HC} is the HC yield, HHV $_{HC}$ is the HHV of the HC, and HHV $_{Feed}$ is the HHV of the feedstock, with all variables on a dry basis. The same equation can be used to determine the energy recovery of the PC and SC phases based on the relative yields and their corresponding energy contents (HHV).

To survey the functional groups on the char surfaces, HC, PC, and SC samples were dried and mixed with approximately 200 mg of KBr at a \sim 1–2:100 sample to KBr ratio. The mixture was pelletized on a Carver press under 6 MPa of pressure and analyzed on a Bruker Vertex 70 Fourier Transform Infrared Spectrometer (FT-IR). Infrared spectra were obtained in diffraction mode with 64 scans at a 4 cm $^{-1}$ resolution over a wavenumber range of 4000 – 400 cm $^{-1}$. Spectra were baseline corrected and normalized to the O–H band between 3000 and 3800 cm $^{-1}$.

Gas chromatography – mass spectrometry (GC–MS) was employed to identify the compounds comprising the secondary char in each of the extracted samples. The solubilized SC samples were mixed with excess anhydrous MgSO₄ to remove water, centrifuged, and the supernatant diluted 1:1 with the same solvent used for the extraction. The solutions were analyzed on a Shimadzu Single Quadrupole Gas Chromatograph-Mass Spectrometer (GCMS-QP2020) with a 30 m long Rxi-5MS capillary column having an internal diameter of 0.25 mm and film thickness of 0.25 μm . The initial oven temperature was 40 °C with an injection temperature of 250 °C and a split ratio of 1:10 using ultra high purity helium as a carrier gas. After a 5-minute residence time the column

temperature was increased at a rate of 2 $^{\circ}$ C/min to 300 $^{\circ}$ C and held for 40 min. Ion source and interface temperatures were set at 230 $^{\circ}$ C and 250 $^{\circ}$ C, respectively. The mass spectrometer scanned from 15 to 500 m/z after a solvent cut time of 6 min. Extracted compounds were identified via a NIST library with greater than 90% match.

3. Results and discussion

A series of carbonization experiments were performed on three representative waste mixtures, denoted as SRU for a mixture of commonly disposed of consumer food items as described in Table 1, BSG for brewers spent grain, and DCW for dairy cheese whey. The three waste mixtures are known to contain different fractions of lipids, proteins, and carbohydrates. Previous studies have determined BSG is largely comprised of lignocellulosic material (~60–70%) with a smaller fraction (~10%) of both protein and lipids (Lynch et al., 2016; Mussatto et al., 2006). Compared to the BSG feedstock, the SRU mixture used in this study has a relatively greater fraction of lipids (29 wt%) and carbohydrates (60 wt%) based on the USDA nutritional database (Ahuja et al., 2018). The third feedstock used in this study, DCW, has the greatest intrinsic moisture content and is estimated to contain 11.5 % protein, 1.4 % lipid, 9.2 % ash, and 77.6 % carbohydrates on a dry basis ("USDA Database," 2020).

3.1. HTC of wet wastes

Mass yields of HC, aqueous, and gas products from HTC are provided in Fig. 1 on a dry basis. HTC of BSG resulted in 15% less solid HC and 19% more aqueous phase product than the SRU-HC. HTC of DCW had the least solid and greatest aqueous phase yield of the three feedstocks. The varying product distributions at identical operating conditions shown in Fig. 1 is consistent with the HTC feedstock dependency shown in numerous studies (Lang et al., 2019, 2018; Saba et al., 2017; Wang et al., 2020). Similar HTC operating conditions have resulted in HC mass yields ranging between 14 and 39% to convert SRU (Sharma and Dubey, 2020; Wang et al., 2020, 2018a, 2018b), 45–58% to convert BSG (Arauzo et al., 2018; Baskyr et al., 2014; de Araújo et al., 2020; Jackowski et al., 2020; Olszewski et al., 2020; Ulbrich et al., 2017), and 46–51% for DCW feedstocks (Escala et al., 2013).

The energy content, represented as a HHV, of both the raw feedstock and HC of different feedstocks is provided in Table 2. Compared to the HHVs for DCW and BSG feedstocks which range between 18 and 20 MJ/kg, SRU has a greater HHV of 26 MJ/kg, which is in agreement with prior studies (Sharma and Dubey, 2020). It is important to note that although SRU resulted in the greatest HHV of the three feedstocks, it also had the least increase in energy content, with DCW and BSG having over a 50% increase relative to their initial feedstocks. This is reflected in the overall energy balance, as the energy densification from the HTC of BSG results in a similar energy recovery as SRU-HC, despite having a reduced HC yield.

Table 2 provides proximate and elemental analysis of both raw feedstocks and HCs, which reveals feedstock-dependent compositional changes. Although SRU-HC is slightly more carbon-rich and DCW-HC is more oxygenated, the HTC process changed all three HC's elemental content to a similar extent. However, changes in the proximate analysis upon carbonization differed with feedstock. HTC of SRU resulted in a relatively small change in FC and VM proximate composition, while HCs from BSG and DCW resulted in 25% less VM and twice as much FC relative to their initial feedstocks. Therefore, although HTC provided similar percentage changes in elemental content, the biochemical composition of the initial feed plays a large role in carbonization, degradation, and hydrolysis rates during hydrothermal treatment (Li et al., 2019).

Comparing the ash content in the initial feedstock relative to the HC after HTC reveals both increasing and decreasing trends depending on the feedstock. SRU was found to have a 56% decrease in ash content,

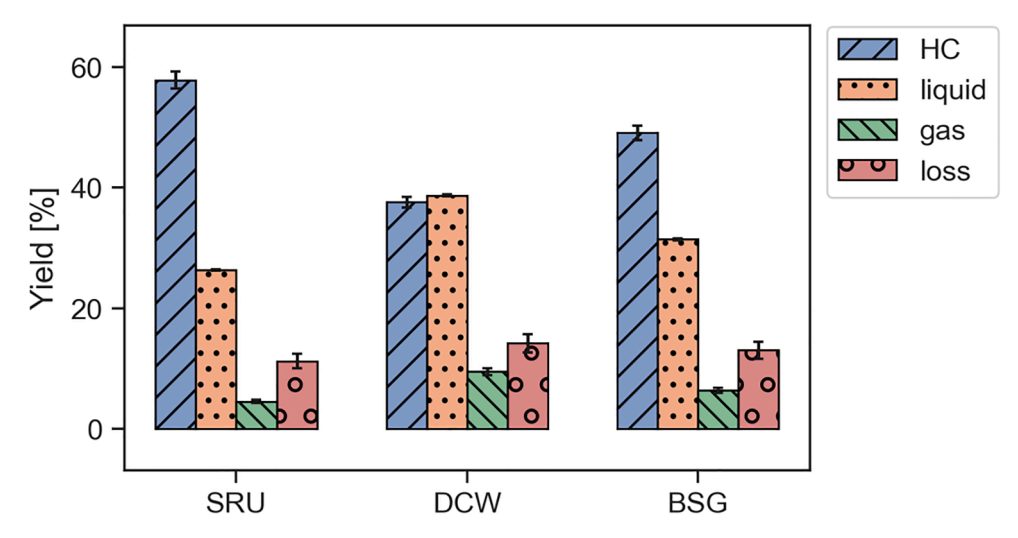


Fig. 1. Mass distribution of products from HTC at 250 °C for 1 hr, including HC, aqueous, and gas phase with different initial feedstocks. The test using SRU was triplicated, and its standard deviation is reported as error bars for al tests.

Table 2Chemical and physical properties of SRU, DCW, and BSG. Moisture is given as received, all other properties on dry basis. Confidence intervals represent standard deviation of duplicates for ash, VM, and FC; or triplicates for moisture, C, H, N, O, HHV. Energy recovery confidence was propagated.

	0,			1 0		
Property	SRU	DCW	BSG	SRU-HC (d.b.)		
Moisture [% wt]	52.9 ± 2.5	94.9 ± 0.1	68.7 ± 0.4	-	-	-
Ash [%wt]	1.4 ± 0.0			$\begin{array}{c} 0.60 \ \pm \\ 0.0 \end{array}$	5.3 ± 0.1	$\begin{array}{c} 1.6 \; \pm \\ 0.0 \end{array}$
VM [%wt]	84.8 \pm	79.5 \pm	85.1 \pm	86.3 \pm	56.6 \pm	64.0 \pm
FC [%wt]	$\begin{array}{c} \textbf{0.8} \\ \textbf{13.8} \ \pm \end{array}$		$\begin{array}{c} 0.6 \\ 15.0 \ \pm \end{array}$			
C [%wt]	$\begin{array}{l} 0.7 \\ 53.9 \ \pm \end{array}$	$\begin{array}{c} \textbf{0.1} \\ \textbf{44.8} \ \pm \end{array}$	$\begin{array}{c} 0.5 \\ 48.8 \ \pm \end{array}$	$\begin{array}{c} 1.2 \\ 75.7 \ \pm \end{array}$	$\begin{array}{c} 0.3 \\ 69.8 \ \pm \end{array}$	$\begin{array}{c} 0.6 \\ 71.5 \ \pm \end{array}$
H [%wt]	$\begin{array}{c} \textbf{2.3} \\ \textbf{8.9} \ \pm \end{array}$	$\begin{array}{c} 0.3 \\ 7.0 \ \pm \end{array}$	$\begin{array}{c} 0.2 \\ 7.4 \ \pm \end{array}$	$\begin{array}{c} 0.2 \\ 10.2 \ \pm \end{array}$	$0.2 \\ 6.0 \pm$	$\begin{array}{c} \textbf{0.2} \\ \textbf{5.7} \ \pm \end{array}$
N [%wt]	$\begin{array}{c} 0.4 \\ 1.7 \ \pm \end{array}$	$\begin{array}{c} 0.1 \\ 2.2 \ \pm \end{array}$	$\begin{array}{c} 0.1 \\ 2.8 \ \pm \end{array}$	$0.2 \\ 1.9 \pm$	0.1 3.5 +	$\begin{array}{c} 0.1 \\ 3.8 \ \pm \end{array}$
O [%wt]	0.1	$0.1 \\ 41.3 \pm$	0.1 38.3 ±	$0.1 \\ 11.5 \pm$	0.0	0.0
	3.0	0.7	0.6	0.5	0.3	0.2
HHV [MJ kg ⁻¹]	$\begin{array}{c} 26.0 \pm \\ 0.3 \end{array}$	0.1	$\begin{array}{c} 19.7 \; \pm \\ 0.2 \end{array}$	0.1	0.2	0.1
Energy Recovery [%]	N/A	N/A	N/A	80.0 ± 1.6	62.0 ± 1.6	72.0 ± 1.5

which would help reduce fouling and slagging risk when combusting the HC within a combustor (Jenkins et al., 1998). A similar reduction in ash content was noted in prior food waste HTC studies with varying compositions (Bhakta Sharma et al., 2021; Gupta et al., 2020; Theppitak et al., 2020). Prior work indicates that the rate of solubilization of ash relative to organics is *writ large* feedstock dependent, (Smith et al., 2016). This likely holds for vastly different sources of food waste (e.g., dairy versus brewery) but that mixtures of retail level food waste (e.g., supermarket, restaurant, or university canteens wastes) may be similar "enough" to show minimal variation in at least proximate analysis, despite global differences in diets.

The extent of organic solubilization contributes to observed changes in HTC product yields and composition. Benchtop studies have characterized two phases of HCs resulting from HTC; a core–shell structure with a more graphitic primary char (PC) coated with a reactive and labile secondary char (SC) phase condensed on the surface of the PC (Lucian et al., 2018). Often, HCs are extracted with solvents (Fang et al.,

2015; Liu et al., 2020) or dried in an oven after HTC (Gupta et al., 2020; Jackowski et al., 2020; Sharma and Dubey, 2020), which can lead to significant variability in apparent char characteristics such as organic recovery rate, heating value and combustion efficiency (Jenkins et al., 1998; Kumar et al., 2020). Structural differences between the residual PC and solvent extracted SC phase may be significant in terms of HTC-to-fuel process decision making.

3.2. Solvent comparison

The amount of PC and SC extracted using the different six solvents are plotted in Fig. 2. The solvent-extracted PC and SC fractions of each HC product are stacked in the same column and denoted with different hatchings. The fraction of extracted SC was the greatest for the alcohol solvents, while relatively nonpolar, hydrophobic DCM and HEX solvents extracted half as much SC, at most. Therefore, the SC fraction was expected to comprise more polar and hydrophilic compounds; similar properties into which it preferentially solvates. This is supported by FTIR analysis of HC, PC, and SC (see supplementary material). In addition, the amount of extractable SC in HC differs by feedstock. HTC of SRU produced the most HC by mass of the three feedstocks, but the least PC by mass of the three feedstocks after every solvent extraction. In contrast, HC from DCW and BSG retain most of their solid mass in the PC phase with minimal extractable SC with DCM and HEX. Therefore, SRU-HC comprises a greater labile fraction of extractable organics that partition into a SC.

The DTG curves of HCs and PCs (see supplementary material) reveal two main peaks in VM region, the first between 150 and 300 °C and the second between 300 and 500 °C. The DTG curves illustrate how the low-temperature volatile nature of SRU-HC is due to labile organics present in the SC. The low-temperature peak corresponds to the considerable fraction of volatile extractables present in the SC phase. In the context of HC being used as a solid fuel, the large quantity of highly volatile compounds can be problematic in combustion scenarios. These compounds devolatilize quickly and potentially lower the flame temperature, leading to poor ignition and incomplete combustion of the solid residue. The two domains shown in the DTG curves have different oxidation rates, which may result in an inefficient overall energy recovery (Jenkins et al., 1998; Muthuraman et al., 2010).

Solvent extractions using HEX and IPA reduce the relative height of the low-temperature peak, similarly to DTG curves of hydrothermally carbonized oil-extracted food wastes (Su et al., 2021). For alcohol solvents, the high-temperature peak becomes the most dominant. The more volatile and oxygenated SC fraction of HC derived from SRU is consistent

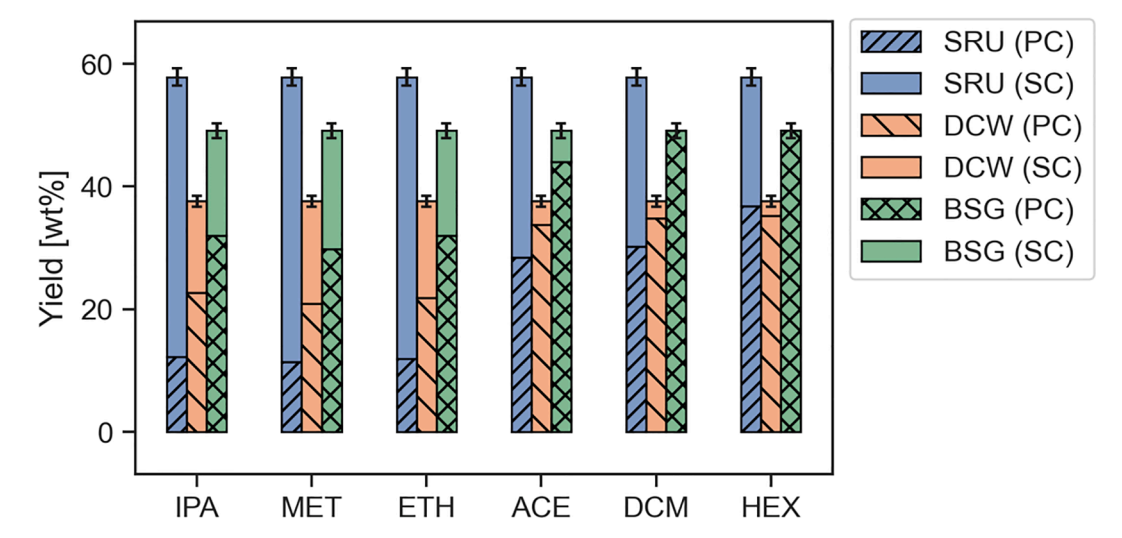


Fig. 2. Distribution of PC and SC in the samples (HCs produced at 250 °C, 1 h using SRU, DCW, and BSG) depending on the solvent used. The sum of PC and SC gives the overall HC yield. Error bars calculated as the standard deviation of HC yield.

with the lighter, hydrophilic fraction identified in other studies (Li et al., 2020; Lucian et al., 2018). Polar solvents best partition HC into two phases having distinct thermal stabilities. The same behavior was found for DCW and BSG, but in these cases the low temperature peak was already smaller than the high-temperature peak, which can be attributed to a lower volatile fraction in the PC due to DCW and BSG lower lipid content, compared to SRU.

HTC solid composition and elemental content was measured after each solvent extraction (see supplementary material), and the percentage change due to extraction is provided in Table 3. The SRU-PC solids have the greatest percent elemental and proximate change of the three feedstocks, consistent with SRU-HC containing the highest mass fraction of extractable products. All extraction solvents led to a more oxygenated and less carbonaceous SRU-PC phase. This relative increase in oxygen content and corresponding decrease in elemental carbon content has the following trend with solvent selection: ACE \approx DCM > MET \approx ETH >HEX \approx IPA. Proximate analysis reveals a differing trend for SRU-PC phases than elemental trends, with a relative decrease in VM and corresponding increase in FC with solvent selection occurring with a trend of: MET \approx ETH \approx ACE > DCM > IPA \approx HEX. The trends seen for SRU-HC are not observed for BSG PCs, which have similar increases in oxygen and decreases in carbon content after solvent extraction, except for HEX. For both DCW-PC and BSG-PC, the relative changes are not as significant as SRU-PC, consistent with the extractability of SC compounds shown in Fig. 2.

Table 3 further shows that solvent extraction reduces the energy content in the SRU-PC phase by approximately 25-28% using ETH, MET, ACE and DCM solvents. For DCW-HC and BSG-HC, solvent extraction led to HHV changes ranging between 2 and 11%. A decrease in HHV in the PC phase suggests that the extracted SC is comprised of more energy dense compounds that can be further used as fuel. To best show the energy content across phases, Table 4 provides energy recoveries of both the PC and SC phases after solvent extraction. Table 4 shows that for HC created from the representative food waste mixture, the SC phase has a higher energy content than the PC phase following extraction with all solvents except HEX, highlighting the poor extractability of this unbranched, relatively nonpolar alkane for SC components. On the other hand, the alcohol extracts from SRU contain more than 70% of the energy content of the initial feedstock; a recovery that is similar to or better than many HTC studies (Sharma and Dubey, 2020; Su et al., 2021; Theppitak et al., 2020). Therefore, alcohol extraction of SRU-HC will effectively partition the as-carbonized HC to an energydense secondary char phase, from which it may be possible to recover liquid fuel precursors.

Table 3Percentage change in chemical and physical properties of HCs after solvent extractionon a dry basis. Confidence intervals are propagated from the standard deviation of duplicates for ash, VM, and FC; or triplicates for C, H, N, O, and HHV.

Sample	Ash	VM	FC	С	Н	N	О	HHV
	[%]	[%]	[%]	[%]	[%]	[%]	[%]	[%]
SRU-PC	426	-35	182	-9	-46	132	54	-26
(MET)	\pm 27	\pm 2	$\pm~26$	$\pm~0$	\pm 2	$\pm~10$	\pm 6	± 2
SRU-PC	277	-33	181	-8	-45	130	53	-25
(ETH)	$\pm~60$	± 1	$\pm~20$	$\pm~0$	\pm 2	$\pm~10$	\pm 5	± 2
SRU-PC	216	-28	154	-6	-39	120	42	-21
(IPA)	$\pm~0$	± 1	$\pm~16$	± 0	± 1	± 6	± 3	± 1
SRU-PC	144	-34	188	-10	-45	131	75	-28
(ACE)	$\pm~10$	± 1	$\pm~21$	$\pm~0$	± 1	\pm 7	\pm 4	± 1
SRU-PC	225	-32	176	-10	-46	137	68	-28
(DCM)	$\pm~12$	± 1	$\pm~20$	$\pm~0$	± 1	± 7	± 7	± 2
SRU-PC	129	-25	144	-6	-34	110	43	-19
(HEX)	± 9	± 1	$\pm~17$	$\pm~0$	± 1	\pm 6	± 2	± 1
DCW-PC	$27 \pm$	-12	$11 \pm$	-2	-19	$13~\pm$	4 ±	$-8~\pm$
(MET)	1	± 0	0	± 0	± 1	0	0	2
DCW-PC	34 \pm	-15	15 \pm	-5	-17	9 ± 0	15	-11
(ETH)	2	± 0	0	$\pm~0$	± 1		± 1	± 2
DCW-PC	15 \pm	-5	4 ± 0	-2	-13	7 ± 0	$8 \pm$	$-6 \pm$
(IPA)	0	± 0		$\pm~0$	± 1		0	2
DCW-PC	24 \pm	-11	9 ± 0	-5	-15	$11~\pm$	19	-11
(ACE)	1	± 0		$\pm~0$	$\pm~0$	0	± 1	± 1
DCW-PC	23 \pm	-10	9 ± 0	-5	-13	9 ± 0	17	$-9 \pm$
(DCM)	1	± 0		$\pm~0$	$\pm~0$		$\pm~0$	1
DCW-PC	14 \pm	-5	3 ± 0	-0	-5	5 ± 0	-2	$-2 \pm$
(HEX)	1	± 0		± 0	$\pm~0$		$\pm~0$	2
BSG-PC	45 \pm	-13	$19 \pm$	-2	-6	6 ± 0	$5 \pm$	$-3 \pm$
(MET)	4	± 1	1	± 0	$\pm~0$		0	1
BSG-PC	$50 \pm$	-13	18 \pm	-2	-6	5 ± 0	$6 \pm$	$-4 \pm$
(ETH)	0	± 0	0	$\pm~0$	$\pm~0$		0	2
BSG-PC	0 ± 0	-4	5 ± 0	-2	0 ± 0	4 ± 0	$6 \pm$	$-2 \pm$
(IPA)		± 0		± 0			0	1
BSG-PC	$50 \pm$	-11	$16 \pm$	-3	-6	4 ± 0	10	$-5~\pm$
(ACE)	6	± 0	0	± 0	$\pm~0$		$\pm~0$	1
BSG-PC	42 \pm	-10	$13 \pm$	-3	0 ± 0	5 ± 0	$7 \pm$	$-3 \pm$
(DCM)	2	± 0	0	$\pm~0$			0	1
BSG-PC	- 2	-3	4 ± 0	-0	8 ± 0	1 ± 0	-1	2 ± 1
(HEX)	$\pm~0$	$\pm \ 0$		$\pm \ 0$			$\pm~0$	

Fig. 3 are representative stacked GC-MS chromatograms of the extracted secondary char from SRU and DCW feeds. Despite the six solvents extract different mass of SC from the same HC (see Fig. 2), the SC compositions is mildly influenced by the solvent selection compared to the feedstock nature. MET has the most significant influence on the SC

Table 4Energy recovery of PC and SC fractions after solvent extraction. Energy recovery calculations based on HHVs estimated using Dulong's formulate from elemental composition.

Extraction Solvent	Energy SRU- PC	Recovery SRU- SC	[ER, %] DCW- PC	DCW- SC	BSG- PC	BSG- SC
Methanol (MET)	12.0	72.8	32.0	28.0	43.6	29.2
Ethanol (ETH)	12.9	71.9	33.0	26.9	46.7	26.1
Isopropyl Alcohol (IPA)	14.1	70.7	35.2	24.8	47.1	25.7
Acetone (ACE)	32.8	52.0	53.1	6.9	64.9	7.9
Dichloromethane (DCM)	35.4	49.4	55.1	4.9	72.8	0.0
Hexane (HEX)	48.8	36.0	56.1	3.9	72.8	0.0

composition, extracting a smaller fraction of C18 oleic acid relative to C14 myristic and C16 palmitic acid (see supplementary material). Concerning the effect of feedstock nature on SC composition, an oleic

acid peak is the most prominent in terms of peak area of all the compounds identified in SC from SRU, while palmitic acid peak is the most prominent peak area in DCW and BSG (see supplementary material). Approximately 68% of the GC-MS peak area is comprised of oleic acid for SRU derived SC phase, while only 8 and 37% of the GC-MS peak area are comprised of oleic acid for extracted secondary chars of DCW and BSG, respectively. The greater long chain fatty acid content identified in the SRU-SC phase, compared to DCW and BSG, is consistent with the hydrolysis of lipids, which are found in high concentrations in U.S. supermarket and food service waste (Lee et al., 2020; Li et al., 2020). These oily compounds have a high energy density (Fassinou, 2012), and can be converted into biodiesel through transesterification (Maghrebi et al., 2021), into diesel-range hydrocarbons through hydrodeoxygenation (Serrano et al., 2019), or into other added value bio-products (e.g. biodiesel cold-properties enhancers, lubricants, fabric conditioners, surfactants, paint driers, vinyl stabilizer, and cosmetics) through isomerization (Maghrebi et al., 2021).

SRU and DCW derived SC show more peaks related to short chain

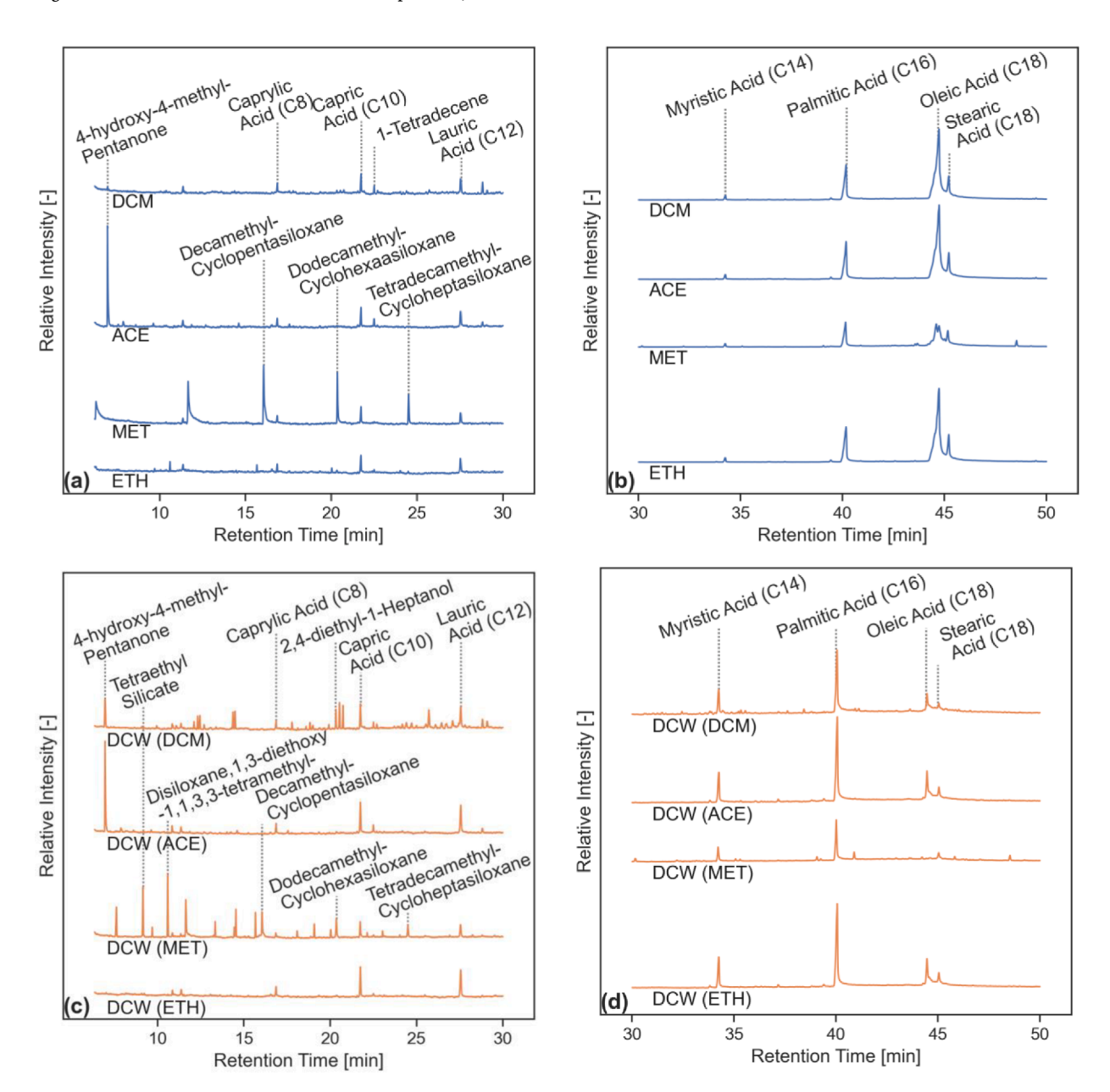


Fig. 3. GC-MS chromatograms for SC extracted using DCM, ACE, MET, and ETH from SRU (a and b) and DCW (c and d), divided in short (a and c), and long retention time regions (b and d).

compounds (Fig. 3) compared to BSG, which can be attributed to their greater carbohydrate and protein contents.

The smaller fraction but similar nature for BSG-SC compared to DCW-SC, suggests this phase derives from the reaction of proteins, carbohydrates, while the lignocellulosic fraction tends to partition in the PC phase.

3.3. Summary of results

HTC effectively converts food waste into a valuable HC that can be separated via solvent extraction into PC and SC. The PC has improved coal-like characteristics with respect to the original HC, and the extracted SC could be used as a source of liquid fuel precursors. Both feedstock nature and solvent selection importantly impact the amount and composition of these phases.

In terms of feedstock composition, the lipid content directly corresponds to an increased production of long chain fatty acids, whereas carbohydrates and proteins favor the production of shorter-chain compounds in the SC. The lignocellulosic fraction preferentially forms PC. Concerning the solvent selection, alcohols extract the largest mass of secondary char among all options. ETH, ACE and DCM maximize the content of long chain fatty acid in the SC and remove the volatilization peak at low temperature visible during PC oxidation that may result in an inefficient overall energy recovery. Also, ETH produce PC with the highest FC fraction among all solvents.

In summary, for lipid-rich substrates like retail level food waste (SRU), up to 50 wt% of the original feedstock can be converted into a SC phase mainly composed of long chain fatty acids using HTC followed by ETH extraction. These compounds represent valuable liquid fuels and chemical precursors, while the solid PC shows improved coal-like characteristics. For carbohydrates and proteins-rich substrates like dairy cheese whey DCW, HTC produces a smaller fraction of SC richer in short chain compounds, while for lignocellulosic ones, it preferentially produces PC. In this case, a solvent extraction using DCM or ACE minimizes the SC mass extracted (thus maximizing the PC one) but removes the low temperature volatilization peak in PC oxidation, possibly avoiding potentially undesirable combustion behavior for the solid PC.

4. Conclusions

Brewer's spent grain, dairy cheese whey and a representative food waste mixture were hydrothermally carbonized. The resulting hydrochars were separated via solvent extraction into a solid primary char and an oily secondary char. Feedstock nature and solvent selection impact the amount and composition of the char phases. For lipid-rich substrates, ethanol separates a secondary char phase rich in fuel precursors from a solid primary char with improved coal-like characteristics. Carbohydrates and proteins-rich substrates produces less secondary char, richer in short chain compounds. Lignocellulosic substrates preferentially produce primary char. Acetone and dichloromethane maximize primary char yield and mitigate potential combustion problems.

CRediT authorship contribution statement

Matteo Pecchi: Methodology, Investigation, Writing – original draft. Marco Baratieri: Supervision. Jillian L. Goldfarb: Conceptualization, Resources, Funding acquisition, Supervision. Alex R. Maag: Methodology, Investigation, Writing – original draft.

Declaration of Competing Interest

The authors declare that they have no known competing financial interests or personal relationships that could have appeared to influence the work reported in this paper.

Acknowledgements

The authors thank Laura G. Falls for her assistance compiling the food waste mixture, Akio Enders for procuring the brewery waste, and Rob Ralyea of Cornell Dairy for the cheese whey.

Funding

This work was partially supported by a Hatch Grant under accession number 1021398 from the USDA National Institute of Food and Agriculture and by the National Science Foundation CBET under award number 2031916.

Appendix A. Supplementary data

Supplementary data to this article can be found online at https://doi.org/10.1016/j.biortech.2022.126799.

References

- Ahuja, J.K.C., Haytowitz, D.B., Pehrsson, P.R., Roseland, J., Exler, J., Khan, M., Nickle, M., Nguyen, Q.A., Patterson, K., Showell, B., Somanchi, M., Thomas, R., Wasswa-Kintu, S., Williams, J., Klingenstein, K., McLean, C., Mille, C., 2018. Composition of Foods: USDA National Nutrient Database for Standard Reference, Legacy (2018), U. S. Department of Agriculture Agricultural Research Service Beltsville Human Nutrition Research Center Nutrient Data Laboratory.
- Arauzo, P., Olszewski, M., Kruse, A., 2018. Hydrothermal carbonization brewer's spent grains with the focus on improving the degradation of the feedstock. Energies 11 (11), 3226. https://doi.org/10.3390/en11113226.
- Baskyr, I., Weiner, B., Riedel, G., Poerschmann, J., Kopinke, F.-D., 2014. Wet oxidation of char-water-slurries from hydrothermal carbonization of paper and brewer's spent grains. Fuel Process. Technol. 128, 425–431. https://doi.org/10.1016/j. fuproc. 2014.07.042.
- Bhakta Sharma, H., Panigrahi, S., Dubey, B.K., 2021. Food waste hydrothermal carbonization: Study on the effects of reaction severities, pelletization and framework development using approaches of the circular economy. Bioresour. Technol. 333, 125187. https://doi.org/10.1016/j.biortech.2021.125187.
- Buzby Jean C., Wells, H.F., Hyman, J., 2014. The Estimated Amount, Value, and Calories of Postharvest Food Losses at the Retail and Consumer Levels in the United States.
- Danso-Boateng, E., Holdich, R.G., Martin, S.J., Shama, G., Wheatley, A.D., 2015. Process energetics for the hydrothermal carbonisation of human faecal wastes. Energy Convers. Manag. 105, 1115–1124. https://doi.org/10.1016/j. enconman.2015.08.064.
- de Araújo, T.P., Quesada, H.B., Bergamasco, R., Vareschini, D.T., de Barros, M.A.S.D., 2020. Activated hydrochar produced from brewer's spent grain and its application in the removal of acetaminophen. Bioresour. Technol. 310, 123399. https://doi.org/ 10.1016/i.biortech.2020.123399.
- Environment Protection Agency, 2018. 2018 Wasted Food Report.
- Escala, M., Graber, A., Junge, R., Koller, C.H., Guiné, V., Krebs, R., 2013. Hydrothermal carbonization of organic material with low dry matter content: The example of waste whey. J. Residuals Sci. Technol. 10, 179–186.
- Fang, J., Gao, B., Chen, J., Zimmerman, A.R., 2015. Hydrochars derived from plant biomass under various conditions: Characterization and potential applications and impacts. Chem. Eng. J. 267, 253–259. https://doi.org/10.1016/j.cej.2015.01.026.
- Fassinou, W.F., 2012. Higher heating value (HHV) of vegetable oils, fats and biodiesels evaluation based on their pure fatty acids' HHV. Energy 45 (1), 798–805. https://doi.org/10.1016/j.energy.2012.07.011.
- Gao, L., Volpe, M., Lucian, M., Fiori, L., Goldfarb, J.L., 2019. Does hydrothermal carbonization as a biomass pretreatment reduce fuel segregation of coal-biomass blends during oxidation? Energy Convers. Manag. 181, 93–104. https://doi.org/ 10.1016/j.enconman.2018.12.009.
- Gupta, D., Mahajani, S.M., Garg, A., 2020. Investigation on hydrochar and macromolecules recovery opportunities from food waste after hydrothermal carbonization. Sci. Total Environ. 749, 142294. https://doi.org/10.1016/j. scitotenv.2020.142294.
- Hitzl, M., Mendez, A., Owsianiak, M., Renz, M., 2018. Making hydrochar suitable for agricultural soil: A thermal treatment to remove organic phytotoxic compounds. J. Environ. Chem. Eng. 6 (6), 7029–7034.
- Jackowski, M., Niedzwiecki, L., Lech, M., Wnukowski, M., Arora, A., Tkaczuk-Serafin, M., Baranowski, M., Krochmalny, K., Veetil, V.K., Seruga, P., Trusek, A., Pawlak-Kruczek, H., 2020. HTC of wet residues of the brewing process: Comprehensive characterization of produced beer, spent grain and valorized residues. Energies 13 (8), 2058. https://doi.org/10.3390/en13082058.
- Jain, A., Balasubramanian, R., Srinivasan, M.P., 2016. Hydrothermal conversion of biomass waste to activated carbon with high porosity: A review. Chem. Eng. J. 283, 789–805. https://doi.org/10.1016/j.cej.2015.08.014.
- Jenkins, B.M., Baxter, L.L., Miles, T.R., Miles, T.R., 1998. Combustion properties of biomass. Fuel Process. Technol. 54 (1-3), 17–46. https://doi.org/10.1016/S0378-3820(97)00059-3.

- Kumar, A., Saini, K., Bhaskar, T., 2020. Hydochar and biochar: Production, physicochemical properties and techno-economic analysis. Bioresour. Technol. 310, 123442. https://doi.org/10.1016/j.biortech.2020.123442.
- Lang, Q., Guo, Y., Zheng, Q., Liu, Z., Gai, C., 2018. Co-hydrothermal carbonization of lignocellulosic biomass and swine manure: Hydrochar properties and heavy metal transformation behavior. Bioresour. Technol. 266, 242–248. https://doi.org/ 10.1016/i.biortech.2018.06.084.
- Lang, Q., Luo, H., Li, Y.i., Li, D., Liu, Z., Yang, T., 2019. Thermal behavior of hydrochar from co-hydrothermal carbonization of swine manure and sawdust: effect of process water recirculation. Sustain. Energy Fuels 3 (9), 2329–2336. https://doi.org/ 10.1039/C9SE00332K.
- Lee, J., Choi, O.K., Oh, D., Lee, K., Park, K.Y., Kim, D., 2020. Stimulation of Lipid Extraction Efficiency from Sewage Sludge for Biodiesel Production through Hydrothermal Pretreatment. Energies 13, 6392. https://doi.org/10.3390/ en13236392
- Li, Y., Liu, H., Xiao, K., Jin, M., Xiao, H., Yao, H., 2020. Combustion and Pyrolysis Characteristics of Hydrochar Prepared by Hydrothermal Carbonization of Typical Food Waste: Influence of Carbohydrates, Proteins, and Lipids. Energy and Fuels 34 (1), 430–439. https://doi.org/10.1021/acs.energyfuels.9b02940.
- Li, Y., Liu, H., Xiao, K., Liu, X., Hu, H., Li, X., Yao, H., 2019. Correlations between the physicochemical properties of hydrochar and specific components of waste lettuce: Influence of moisture, carbohydrates, proteins and lipids. Bioresour. Technol. 272, 482–488. https://doi.org/10.1016/j.biortech.2018.10.066.
- Libra, J.A., Ro, K.S., Kammann, C., Funke, A., Berge, N.D., Neubauer, Y., Titirici, M.-M., Fühner, C., Bens, O., Kern, J., Emmerich, K.-H., 2011. Hydrothermal carbonization of biomass residuals: a comparative review of the chemistry, processes and applications of wet and dry pyrolysis. Biofuels 2 (1), 71–106. https://doi.org/ 10.4155/bfs.10.81.
- Liu, X., Zhai, Y., Li, S., Wang, B., Wang, T., Liu, Y., Qiu, Z., Li, C., 2020. Hydrothermal carbonization of sewage sludge: Effect of feed-water pH on hydrochar's physicochemical properties, organic component and thermal behavior. J. Hazard. Mater. 388, 122084. https://doi.org/10.1016/j.jhazmat.2020.122084.
- Liu, Z., Quek, A., Balasubramanian, R., 2014. Preparation and characterization of fuel pellets from woody biomass, agro-residues and their corresponding hydrochars. Appl. Energy 113, 1315–1322. https://doi.org/10.1016/j.apenergy.2013.08.087.
- Lucian, M., Volpe, M., Gao, L., Piro, G., Goldfarb, J.L., Fiori, L., 2018. Impact of hydrothermal carbonization conditions on the formation of hydrochars and secondary chars from the organic fraction of municipal solid waste. Fuel 233, 257–268. https://doi.org/10.1016/j.fuel.2018.06.060.
- Lynch, K.M., Steffen, E.J., Arendt, E.K., 2016. Brewers' spent grain: a review with an emphasis on food and health. J. Inst. Brew. 122 (4), 553–568. https://doi.org/ 10.1002/jib.363.
- Maghrebi, R., Buffi, M., Bondioli, P., Chiaramonti, D., 2021. Isomerization of long-chain fatty acids and long-chain hydrocarbons: A review. Renew. Sustain. Energy Rev. 149, 111264. https://doi.org/10.1016/j.rser.2021.111264.
- Mihajlović, M., Petrović, J., Maletić, S., Isakovski, M.K., Stojanović, M., Lopičić, Z., Trifunović, S., 2018. Hydrothermal carbonization of Miscanthus × giganteus: Structural and fuel properties of hydrochars and organic profile with the ecotoxicological assessment of the liquid phase. Energy Convers. Manag. 159, 254–263. https://doi.org/10.1016/j.enconman.2018.01.003.
- Mussatto, S.I., Dragone, G., Roberto, I.C., 2006. Brewers' spent grain: generation, characteristics and potential applications. J. Cereal Sci. 43 (1), 1–14. https://doi. org/10.1016/j.jcs.2005.06.001.

- Muthuraman, M., Namioka, T., Yoshikawa, K., 2010. Characteristics of co-combustion and kinetic study on hydrothermally treated municipal solid waste with different rank coals: A thermogravimetric analysis. Appl. Energy 87 (1), 141–148. https://doi. org/10.1016/j.apenergy.2009.08.004.
- Olszewski, M.P., Nicolae, S.A., Arauzo, P.J., Titirici, M.-M., Kruse, A., 2020. Wet and dry? Influence of hydrothermal carbonization on the pyrolysis of spent grains. J. Clean. Prod. 260, 121101. https://doi.org/10.1016/j.jclepro.2020.121101.
- Saba, A., Saha, P., Reza, M.T., 2017. Co-Hydrothermal Carbonization of coal-biomass blend: Influence of temperature on solid fuel properties. Fuel Process. Technol. 167, 711–720. https://doi.org/10.1016/j.fuproc.2017.08.016.
- Serrano, D.P., Escola, J.M., Briones, L., Arroyo, M., 2019. Selective hydrodecarboxylation of fatty acids into long-chain hydrocarbons catalyzed by Pd/Al-SBA-15. Microporous Mesoporous Mater. 280, 88–96. https://doi.org/10.1016/j.micromeso.2019.01.045.
- Sharma, H.B., Dubey, B.K., 2020. Co-hydrothermal carbonization of food waste with yard waste for solid biofuel production: Hydrochar characterization and its pelletization. Waste Manag. 118, 521–533. https://doi.org/10.1016/j. wasman. 2020.09.009
- Smith, A.M., Singh, S., Ross, A.B., 2016. Fate of inorganic material during hydrothermal carbonisation of biomass: Influence of feedstock on combustion behaviour of hydrochar. Fuel 169, 135–145. https://doi.org/10.1016/j.fuel.2015.12.006.
- Su, H., Zhou, X., Zheng, R., Zhou, Z., Zhang, Y., Zhu, G., Yu, C., Hantoko, D., Yan, M.i., 2021. Hydrothermal carbonization of food waste after oil extraction pre-treatment: Study on hydrochar fuel characteristics, combustion behavior, and removal behavior of sodium and potassium. Sci. Total Environ. 754, 142192. https://doi.org/10.1016/ i.scitotenv.2020.142192.
- Theppitak, S., Hungwe, D., Ding, L.u., Xin, D., Yu, G., Yoshikawa, K., 2020. Comparison on solid biofuel production from wet and dry carbonization processes of food wastes. Appl. Energy 272, 115264. https://doi.org/10.1016/j.apenergy.2020.115264.
- Ulbrich, M., Preßl, D., Fendt, S., Gaderer, M., Spliethoff, H., 2017. Impact of HTC reaction conditions on the hydrochar properties and CO2 gasification properties of spent grains. Fuel Process. Technol. 167, 663–669. https://doi.org/10.1016/j. fuproc.2017.08.010.
- USDA Database [WWW Document], 2020. URL https://ndb.nal.usda.gov/fdc-app. html#/food-details/170885/nutrients (accessed 10.8.20).
- Volpe, M., Goldfarb, J.L., Fiori, L., 2018. Hydrothermal carbonization of Opuntia ficusindica cladodes: Role of process parameters on hydrochar properties. Bioresour. Technol. 247, 310–318. https://doi.org/10.1016/j.biortech.2017.09.072.
- Wang, T., Si, B., Gong, Z., Zhai, Y., Cao, M., Peng, C., 2020. Co-hydrothermal carbonization of food waste-woody sawdust blend: Interaction effects on the hydrochar properties and nutrients characteristics. Bioresour. Technol. 316, 123900. https://doi.org/10.1016/j.biortech.2020.123900.
- Wang, T., Zhai, Y., Li, H., Zhu, Y., Li, S., Peng, C., Wang, B., Wang, Z., Xi, Y., Wang, S., Li, C., 2018a. Co-hydrothermal carbonization of food waste-woody biomass blend towards biofuel pellets production. Bioresour. Technol. 267, 371–377. https://doi.org/10.1016/j.biortech.2018.07.059.
- Wang, T., Zhai, Y., Zhu, Y., Peng, C., Xu, B., Wang, T., Li, C., Zeng, G., 2018b. Influence of temperature on nitrogen fate during hydrothermal carbonization of food waste. Bioresour. Technol. 247, 182–189. https://doi.org/10.1016/j.biortech.2017.09.076.
- Zhang, X., Gao, B., Fang, J., Zou, W., Dong, L., Cao, C., Zhang, J., Li, Y., Wang, H., 2019. Chemically activated hydrochar as an effective adsorbent for volatile organic compounds (VOCs). Chemosphere 218, 680–686. https://doi.org/10.1016/j. chemosphere.2018.11.144.